

First-principles study of the ferroelastic phase transition in CaCl_2

J.A. Válgora, J.M. Pérez-Mato, and Alberto García*

Departamento de Física de la Materia Condensada,
Universidad del País Vasco, Apartado 644, 48080 Bilbao, Spain

K. Schwarz and P. Blaha

Institute of Physical and Theoretical Chemistry, Vienna University
of Technology, A-1060 Vienna, Getreidemarkt 9/156, Austria

First-principles density-functional calculations within the local-density approximation and the pseudopotential approach are used to study and characterize the ferroelastic phase transition in calcium chloride (CaCl_2). In accord with experiment, the energy map of CaCl_2 has the typical features of a pseudoproper ferroelastic with an optical instability as ultimate origin of the phase transition. This unstable optic mode is close to a pure rigid unit mode of the framework of chlorine atoms and has a negative Grüneisen parameter. The ab-initio ground state agrees fairly well with the experimental low temperature structure extrapolated at 0 K. The calculated energy map around the ground state is interpreted as an extrapolated Landau free-energy and is successfully used to explain some of the observed thermal properties. Higher-order anharmonic couplings between the strain and the unstable optic mode, proposed in previous literature as important terms to explain the soft-phonon temperature behavior, are shown to be irrelevant for this purpose. The LAPW method is shown to reproduce the plane-wave results in CaCl_2 within the precision of the calculations, and is used to analyze the relative stability of different phases in CaCl_2 and the chemically similar compound SrCl_2 .

I. INTRODUCTION

In recent years, ab-initio methods based on density-functional theory have been shown to have predictive power in the field of thermal structural phase transitions. In particular, first-principles calculations within the local-density approximation (LDA) have been able to reproduce ferroelectric and other instabilities in perovskite oxides such as BaTiO_3 , PbTiO_3 or SrTiO_3 .^{1,2,3,4,5} These ab-initio calculations correctly predict a low-symmetry distorted ground state and the eigenvector of the associated distorting mode. Moreover, the ab-initio exploration of the energy around this ground state for the relevant degrees of freedom allows, in general, a parametrization of the obtained energy map as an effective hamiltonian. Thermal effects investigated through Monte Carlo or Molecular Dynamics simulations restricted to this effective hamiltonian show a fair agreement with experiment.

However, the field of temperature-driven ferroelastic phase transitions, where some spontaneous strain component can be identified with the order parameter (proper ferroelastic) or is bilinearly coupled with it (pseudoproper ferroelastic), represents a particular challenge for first-principles calculations. Density-functional methods are known to have accuracy problems when reproducing elastic properties, while in ferroelastics the elastic energy plays a fundamental role in the structural instability.

We report here the results of an ab-initio study of the ferroelastic instability in CaCl_2 based on the density-functional theory within the LDA. A brief preliminary account was presented in Ref. 6. To our knowledge, this is the first study of this type in a ferroelastic temperature-driven system, and can be considered a benchmark of the

capability of these ab-initio methods to reproduce ferroelastic structural instabilities. The case of CaCl_2 is particularly simple: having a rutile-type structure, it undergoes a tetragonal-orthorhombic transition which is well characterized as pseudoproper ferroelastic.^{7,8} The order parameter is one-dimensional and the eigenvector of the unstable optic mode is fully determined by symmetry arguments. This allows an investigation of the origin of the structural instability by considering only a few degrees of freedom of the structure. In comparison with the case of the ferroelectric perovskites, another simplifying feature is the fact that the unstable mode is non-polar, so it is not necessary to include long-range dipolar interactions in any subsequent modeling of the relevant degrees of freedom as a local-mode effective hamiltonian.

In this work, the existence of an orthorhombic (slightly distorted rutile structure) ground-state of the system is explored, and the total energy is parametrized as a function of the relevant degrees of freedom. Special emphasis is put on a comparison of the resulting energy map with a temperature dependent Landau potential, and the resulting experimental behavior. We also investigate the importance of other secondary degrees of freedom.

The paper is organized as follows. In Sec. II we describe the computational details of the first-principles calculations. In Sec. III we present the ground state of CaCl_2 obtained from our ab-initio calculations and its comparison with experiment. Temperature effects are discussed in detail in Sec. IV. In Sec. V we demonstrate the importance of secondary degrees of freedom in the determination of the ground state of the system and present the results obtained from a direct ab-initio minimization of the orthorhombic structure of CaCl_2 . The effects of external stresses exerted on CaCl_2 are

also considered. Most of the calculations were performed with a pseudopotential method but the results were cross checked against the highly accurate all-electron linearized augmented plane wave (LAPW) method. The latter was mainly used to study the relative energies between the experimental CaCl_2 structure and the denser-packed fluorite-type structure in both CaCl_2 and SrCl_2 . In Sec. VI we discuss the competition between the three different structures (fluorite-type, rutile-type and orthorhombic CaCl_2 -type). Finally we draw some relevant conclusions in Sec. VII.

II. DETAILS OF THE AB-INITIO CALCULATIONS

Part of the calculations presented in this paper were performed using density-functional theory within the pseudopotential approach with plane waves (PW). For these the exchange-correlation energy was evaluated within the local-density approximation, (LDA)^{9,10} using the Perdew and Zunger parametrization¹¹ of the Ceperley and Alder¹² interpolation formula for a homogeneous electron gas. First-principles norm-conserving pseudopotentials for Ca and Cl were generated using the scheme proposed by Troullier and Martins.¹³ The Ca pseudopotential was calculated with a nonlinear core correction in the $3d^{0.20}4s^{0.50}4p^{0.15}$ non-spin-polarized valence configuration, with cutoff radii (in bohr) $r_{cd} = 1.29$, $r_{cs} = 2.66$, and $r_{cp} = 3.09$. The Cl pseudopotential was calculated in the $3s^{2.00}3p^{4.50}3d^{0.50}$ non-spin-polarized valence configuration with cutoff radii $r_{cs} = 1.72$, $r_{cp} = 1.48$, and $r_{cd} = 2.21$. A plane-wave basis set up to a kinetic energy cutoff of 25 ryd and a $4 \times 4 \times 5$ Monkhorst-Pack¹⁴ shifted k-point sampling in the Brillouin zone (BZ) were considered. Both the basis set and k-point sampling were successfully tested to give converged total energies. A modified Broyden method¹⁵ was used for the simultaneous relaxation of the ions and the unit cell while the symmetry was preserved. Relaxation of the free atomic coordinates was considered accomplished when atomic forces were less than 0.05 mhartree/bohr, and the unit-cell relaxation stopped when the stresses were smaller than 1 MPa.

The full-potential LAPW method as implemented in the WIEN97 program¹⁶ was used to obtain the results presented in Sec. VI. The “muffin tin” radius was chosen to be 2.3 bohr for all atoms involved in the present calculations. The maximum number of plane waves is determined by the parameter $R_{\text{mt}}K_{\text{max}}$, which was 8 in our calculations (R_{mt} is the radius of the atomic sphere and K_{max} is the largest reciprocal wavevector used in the LAPW basis set). This led to about 1000 plane waves to describe the valence and semi-core states. Local orbitals were used to treat the Ca $3s, 3p$ and Cl $3s$ semi-core states. The density of the core electrons was computed in the crystal potential of each iteration in the self-consistent cycles (thawed core). Exchange and cor-

relation was treated within the LDA using the Perdew and Wang parametrization¹⁷ of the Ceperley and Alder data. For tetragonal and orthorhombic structures we took a $5 \times 5 \times 8$ Monkhorst-Pack shifted k-point sampling in the BZ to give converged total energies, and a $12 \times 12 \times 12$ sampling for cubic structures. Self-consistency was reached when the total energy of consecutive iterations changed by less than 0.01 mhartree. The forces were computed according to Kohler et al.¹⁸ and relaxation of the free atomic coordinates was completed when the atomic forces were less than 0.5 mhartree/bohr.

III. THE FERROELASTIC GROUND STATE OF CaCl_2

CaCl_2 undergoes a second order ferroelastic phase transition at 491K from a high-temperature tetragonal rutile-type structure (space group $P4_2/mnm$, $Z = 2$) to an orthorhombic one (space group $Pnnm$, $Z = 2$). The phase transition is therefore equitranslational, with an order parameter of B_{1g} symmetry (antisymmetric for operations 4 and m_{xy}). This is in fact the symmetry of the orthorhombic spontaneous strain $\epsilon = (\epsilon_1 - \epsilon_2)/2$. The tetragonal high-temperature structure has also a single optical mode of B_{1g} symmetry, which according to spectroscopic observations strongly softens as the temperature is lowered and causes the structural instability.⁷ Thus, the case of CaCl_2 is a textbook example of a pseudoproper ferroelastic transition, where the actual order parameter Q is the amplitude of an optical mode, while the spontaneous strain, being of the same symmetry, is bilinearly coupled to it.

We started the ab-initio analysis by searching for the tetragonal rutile-type structure of minimal energy, henceforth called the (ab-initio) parent structure. The atomic positions, constrained within the symmetry $P4_2/mnm$ (a single free atomic parameter), and the ratio c/a of the tetragonal unit cell were relaxed for different unit cell volumes. For each volume the total energy of the relaxed structure was calculated and the corresponding results were fitted using the Murnaghan equation of state¹⁹ to obtain the volume of the $P4_2/mnm$ structure of minimal energy. The calculated parent structure is compared in Table I with the experimental high-temperature structure extrapolated at 0 K.²⁰ The agreement between PW and experiment is remarkable considering that LDA is known to underestimate unit cell volumes and thermal effects influence the experimental high-temperature structure. Also shown in the table are the structural parameters obtained using the LAPW method. The deviation between PW and LAPW, both using the LDA, is most likely caused by the different treatment of the Ca- $3p$ semi-core states: indirectly through the use of non-linear core corrections in PW, and properly in LAPW.

A sketch of the structure is shown in Fig. 1. Each calcium cation is surrounded by a distorted octahedron of chlorine anions of mmm symmetry. Ideal octahedral

TABLE I: Computed structural parameters and bulk modulus for tetragonal CaCl_2 compared with the experimental values extrapolated to 0 K (Ref. 20). The x atomic coordinate of the Cl atom at 500 K is given in lattice units. We include both PW and LAPW results for comparison.

	PW	Experiment	Diff. (%)	LAPW
$a(\text{\AA})$	6.302	6.343	1	6.242
$c(\text{\AA})$	4.117	4.142	1	4.068
$x(\text{Cl})$	0.3028	0.3040	0.4	0.3032
$B_0(\text{GPa})$	39			41

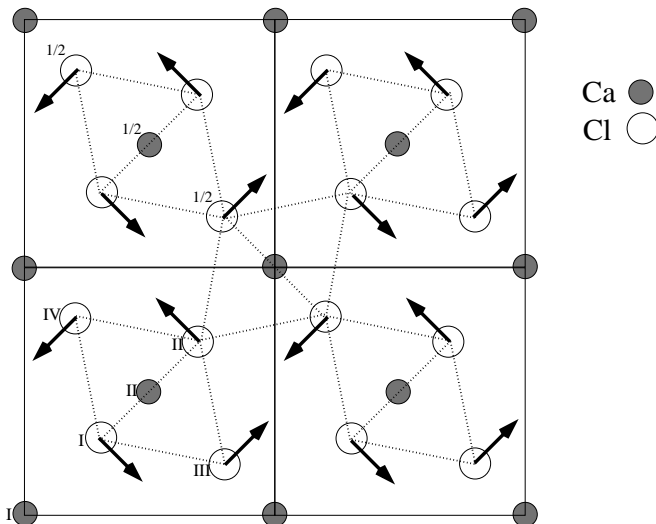


FIG. 1: Sketch showing the parent structure of CaCl_2 and the eigenvector of the unstable B_{1g} mode viewed down the z axis. The mode is close to a rotation around the z axis of the CaCl_6 octahedra as rigid units.

coordination would require $c/a = 2 - \sqrt{2} = 0.5858$ and $x = (2 - \sqrt{2})/2 = 0.2929$ as compared with values of 0.6533 and 0.3028 for our parent structure. This typical distortion of anion octahedra in rutile type structures has been explained as a simple mechanism for maximizing the anion-anion distance, which minimizes its repulsion energy (maximum volume per unit cell), while keeping fixed the cation-anion distances.²¹ Indeed, the unit cell volume of the rutile structure would be maximal under these constraints for $c/a = 0.6325$ and $x = 0.3000$,²¹ in fair agreement with the values calculated ab-initio here and those experimentally observed in CaCl_2 and other rutile structures, including rather less ionic ones.²²

The stability of this ab-initio rutile parent structure with respect to zone-center distortions was then investigated by computing the normal mode frequencies at the Γ point. All Γ modes have real frequencies except the mode of B_{1g} symmetry, confirming the latter's intrinsic instability (see Table II). The frequencies of the stable modes agree fairly well with experimental frequencies; deviations of 10% are to be considered normal if it is taken into account that we are comparing 0 K calculations with experimental values in a structure stabilized at high tem-

TABLE II: Calculated frequencies (given in cm^{-1}) of all zone-center phonons of tetragonal CaCl_2 compared with the available (Raman-active) experimental frequencies (taken from Ref. 7).

irrep	Theory	Exp.(600K)	Diff. (%)
A_{1g}	229.1	203.0	12
A_{2g}	92.7		
B_{1g}	31.5i	17.1	
B_{2g}	261.2	246.7	6
E_g	169.8	150.0	13
A_{2u}	248.7		
B_{1u}	71.0, 257.5		
E_u	76.6, 231.6, 271.0		

peratures. The B_{1g} mode has rather low frequencies in many other rutile-type materials and often exhibits a strong temperature variation, but in most systems is stable at all temperatures.^{23,24} In some compounds it can be destabilized via pressure.^{25,26,27} Obviously, in the case of CaCl_2 , the “soft” behavior of this mode is so extreme that it is unstable at low temperatures. Our calculations, which in principle explore the configuration space at 0 K, agree with this experimental fact. The tendency of the B_{1g} mode to be rather soft can be qualitatively explained by its “quasi rigid-unit” nature. Indeed, the mode is close to a pure rigid unit rotation of the columns (parallel to [001]) of distorted chlorine octahedra forming the structure. Each such column shares corners with four neighboring chains (see Fig. 1), so it can be termed a “quasi rigid unit mode” (QRUM).²⁸ This can be easily checked using the CRUSH package.^{29,30} In fact, the B_{1g} mode does not correspond exactly to a pure rigid unit rotation around the z axis due to the different lengths of the rotation radius of the chlorine atoms in the CaCl_6 octahedra. Ab-initio studies of Karki et al.³¹ show an equivalent situation for the pressure-induced phase transition in stishovite.

Volume effects on the B_{1g} mode frequency were also calculated. The mode has a negative Grüneisen parameter of around -15 , which is in accord with experimental values in other rutile-type compounds.^{32,33,34} The resulting decrease of the mode frequency with pressure is also a typical feature of RUMs and QRUMs, and is the reason why in other rutile-type compounds like rutile itself or stishovite the B_{1g} instability can be attained at high pressures.

Fig. 2 shows the total energy as a function of the amplitude Q of the mode B_{1g} , while maintaining the rest of the structural parameters at their parent-structure values. The eigenvector of this mode (see Fig. 1) has the form $1/\sqrt{8}(000; 000; 1\bar{1}0; \bar{1}10; 110; \bar{1}\bar{1}0)$, where the displacement vectors are listed in the order $(e(\text{Ca}^I), e(\text{Ca}^{II}), e(\text{Cl}^I), e(\text{Cl}^{II}), e(\text{Cl}^{III}), e(\text{Cl}^{IV}))$ (atomic labels are indicated in Fig. 1). The resulting double-well energy map with a minima of 0.44 mhartree can be well fitted using a minimal expansion $E = E_0 +$

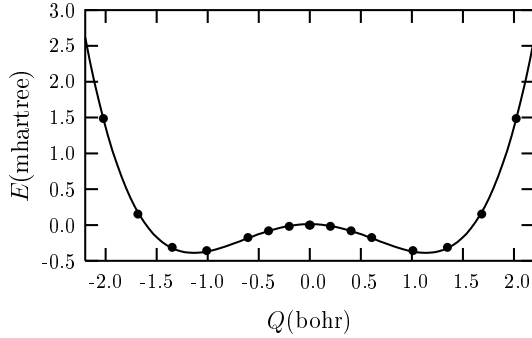


FIG. 2: Total energy (per unit cell) of CaCl_2 as a function of the amplitude Q of the B_{1g} mode. The solid line represents the double-well fit indicated in the text.

$1/2\kappa Q^2 + 1/4\alpha Q^4$, with a mode amplitude of 1.15 bohr at the well minima. The search for the actual ground state requires, however, an exploration of the energy of the system as a function of both Q and the orthorhombic strain, with which it can be bilinearly coupled. In general, the energy map $E(Q, \epsilon)$ around the parent tetragonal configuration can be expanded in the form:

$$E = E_0 + \frac{1}{2}\kappa Q^2 + \frac{1}{4}\alpha Q^4 + \frac{1}{2}C_0\epsilon^2 + \gamma Q\epsilon + \gamma' Q^3\epsilon. \quad (1)$$

Here C_0 is the bare elastic constant of the orthorhombic strain ϵ and corresponds to $2(C_{11} - C_{12})$. We have included only harmonic terms for the elastic energy, but a higher-order coupling term $Q^3\epsilon$ is also included as it will be shown below to be significant. All coefficients in this energy expansion can be determined from ab-initio calculations: κ and α from the above mentioned fit of the double well of Fig. 2 and the bare elastic constant C_0 from the parabolic fit of the total energy calculated as a function of the strain ϵ at $Q = 0$ (see Fig. 3a). The coupling coefficients γ and γ' can be obtained from the fit of the calculated ϵ -conjugate stress $\partial E / \partial \epsilon$ ($\sigma_1 - \sigma_2$) vs. Q at $\epsilon = 0$ (see Fig. 3b) to the expected behavior $\gamma Q + \gamma' Q^3$. In Fig. 3b, deviations from the linear behavior are clearly observed, so the higher non-linear coupling $Q^3\epsilon$ is quite significant. Table III lists the values obtained for these various coefficients. The resulting energy map $E(Q, \epsilon)$, has three stationary points: the saddle point at $Q_0 = 0$, $\epsilon_0 = 0$, corresponds to the unstable tetragonal structure, and the other two symmetry-equivalent stationary points locate the ground state of the structure at the twin related absolute minima $(Q_m, \epsilon_m) = \pm(1.27 \text{ bohr}, 0.029)$. The depth of the minima with respect to the tetragonal parent structure is 0.70 mhartree. When compared with the relative minimum along Q , it means that nearly 50% of the energy minimization corresponds to strain relaxation. This should be compared with the experimental B_{1g} distortion extrapolated to 0 K. According to Ref. 20, the strain ϵ at room temperature is 0.014, and the experimental curve $\epsilon(T)$ can be extrapolated to $\epsilon(0) = 0.022$.

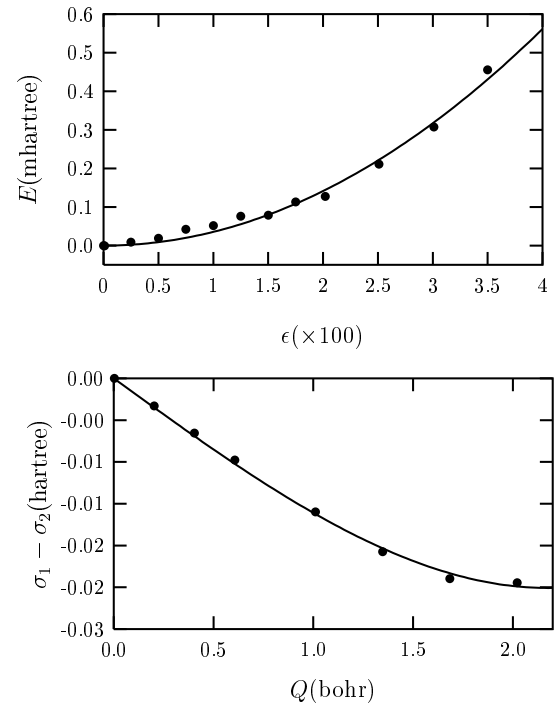


FIG. 3: Upper panel: Fit of the calculated total energy for different strained unit cells to obtain the bare elastic constant C_0 . Lower panel: Calculated $\sigma_1 - \sigma_2$ stress as a function of the amplitude Q of the B_{1g} mode at $\epsilon = 0$, and the corresponding fit to $\gamma Q + \gamma' Q^3$.

TABLE III: Parameters of the total energy expansions $E(Q, \epsilon)$ given in Eq. (1) and Eq. (2).

κ	B_{1g} -mode		A_{1g} -mode		1.01	mh/bohr^4
	-1.33	mh/bohr^2	α	70.42	mh/bohr^2	
Couplings						
γ	-16.6	mh/bohr	γ'	50	mh/bohr	$0.80 \text{ mh}/\text{bohr}^3$
a	50	mh/bohr	b	-1.07	mh/bohr^3	$-194 \text{ mh}/\text{bohr}$
a'	-1.07	mh/bohr^3	b'	16.8	mh/bohr^2	$32.1 \text{ mh}/\text{bohr}^2$
c'	16.8	mh/bohr^2				
Elastic						
C_0	0.68	h (18GPa)	C_+		6.95	h (184GPa)
C_3	3.15	h (83GPa)	C_{+3}		2.15	h (57GPa)

Assuming an analogous behavior for $Q(T)$, as expected in pseudoproper ferroelastics, the experimental value of 0.85 bohr for Q at room temperature²⁰ can be extrapolated to 1.33 bohr at 0 K. This value is in excellent agreement with the ab-initio value while, on the other hand, the orthorhombic ab-initio strain is about 30% overestimated.

IV. TEMPERATURE EFFECTS

The calculated energy map $E(Q, \epsilon)$ can be used as the starting point for the “prediction” of thermal behavior, including the phase transition. This can be done, for instance, through the construction of an effective hamiltonian consistent with the energetics described by $E(Q, \epsilon)$, and its further analysis through Monte Carlo simulations.¹ As a zeroth-order approximation, however, we can already perform some sensible comparisons with experimental results, if we note that the energy map $E(Q, \epsilon)$ can be taken as an approximation for the free-energy (for given Q and ϵ , in the sense of a Landau potential) at 0 K, and we make the (rather drastic) assumption that the temperature effects are restricted to the thermal renormalization up to positive values of the quadratic κ coefficient, so that it follows a Landau type law $\kappa \propto (T - T_0)$. In other words, the coefficients in Table III can be considered an estimation of the coefficients in the Landau free energy, except for κ . For instance, according to Eq. (1), the actual observable elastic constant corresponding to ϵ should soften according to the law: $C(T) = C_0 - \gamma^2/\kappa(T)$, so that the phase transition takes place when $C(T)$ becomes zero at $\kappa(T_c) = \gamma^2/C_0$. According to the parameter values of Table III, this would correspond to a value of $\kappa(T_c) = 0.41$ mhartree/bohr² which, taking into account the effective mass of the mode (m_{Cl} in our Q units) represents a mode frequency $\omega_{B_{1g}} = 17 \text{ cm}^{-1}$, in good agreement with the experimental value⁷ of 14 cm^{-1} .

An expansion of the free energy including a higher-order coupling term $Q^3\epsilon$ as that given in Eq. (1) for $E(Q, \epsilon)$, was proposed to study the temperature behavior of the soft optic phonon observed by Raman spectroscopy experiments.⁷ In particular, this coupling term was included to explain the large value of the slope ratio r of $\omega^2(T)$ below and above the phase transition, as compared to the value of -2 expected from the simplest Landau expansion. By using this extended free-energy expansion, it was demonstrated that the slope ratio of $\omega^2(T)$ is no longer -2 (the mean-field value), but a function which depends on the free-energy expansion coefficients: $r = (k - 4\alpha)/2(\alpha - k)$, where $k = 4\gamma\gamma'/C_0$.⁷ Using this result, the calculated non-linear coupling coefficient γ' predicts a slope ratio of $\omega^2(T)$ of -1.9 , which is not only quite far from the observed r of -6.5 , but it corrects the classical value -2 in the opposite direction. Trying to explain such a slope ratio through this non-linear term in the free energy would require a coefficient γ' one order of magnitude larger than the ab-initio calculated value and of opposite sign, which seems difficult to accept even considering any reasonable thermal renormalization effect. Therefore, our results indicate that this non-classical slope ratio must have a quite different origin. In this respect, it is quite interesting to compare the values of ω^2 at 0 K extrapolated from the experimental linear behavior of $\omega^2(T)$, below T_c (see Fig. 4), with the theoretical expected value ob-

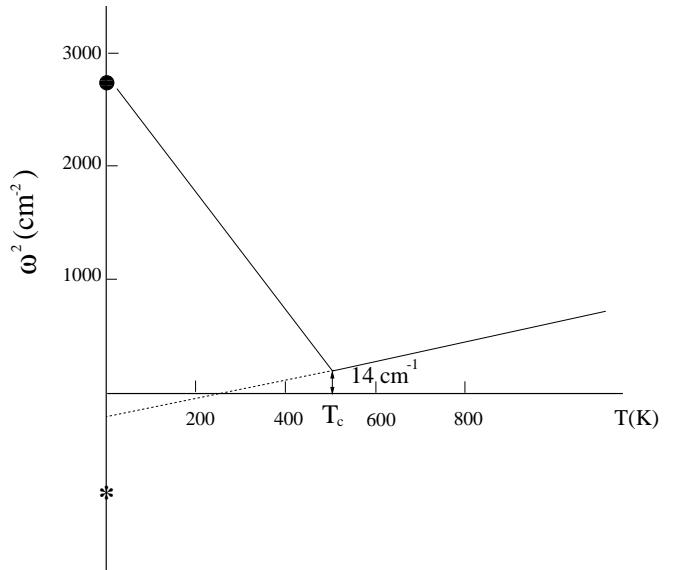


FIG. 4: Sketch of the experimental temperature behavior of the square of the frequency of the soft mode in CaCl₂ (Ref. 7). The asterisk and the black circle at 0 K represent ab-initio values of ω^2 for $Q=0$, $\epsilon=0$ and at the absolute minima of the total-energy map, respectively.

tained from the curvature along Q at the absolute minima of the ab-initio energy map. The experimental value is 3.74 mhartree/bohr² (2790 cm^{-2}) and the theoretical one $\kappa + 3\alpha Q_m^2 + 6\gamma'\epsilon_m Q_m = 3.73$ mhartree/bohr² (2780 cm^{-2}), a surprising excellent agreement. This suggests that the strong slope change of the linear temperature behavior of the mode frequency has a rather simple origin: the Q -stiffness coefficient approaches linearly the ground state value once the system is below T_c . This implies, in general, a correction to the usual Landau description through a change of slope of the linear decrease of the quadratic order parameter coefficient around T_c . This kind of behavior has been actually observed in Monte Carlo simulations of the Φ^4 model when described by means of an effective Landau potential.^{35,36,37} The curvature along Q at the tetragonal maximum is -990 cm^{-2} , indicated in Fig. 4 with an asterisk. This is four times lower than the extrapolated value from the experimental linear behavior of $\omega^2(T)$ above T_c . The deviation of this extrapolated value from the actual 0 K value is also normal in simplified models like the Φ^4 , and is related to the displacive degree of the transition. Only in the displacive limit would one expect both values to agree.^{36,38} A deviation factor of four would correspond to a quite normal and realistic intermediate regime where couplings and ground state energy scales are of the same order of magnitude.

V. SECONDARY DEGREES OF FREEDOM

Until now, in our analysis of the energy we have only considered the primary degrees of freedom which determine the symmetry of the crystal below the transition, i.e., we have expanded the energy only in terms of the amplitude Q of the optic mode B_{1g} and the orthorhombic strain ϵ . However, we must also consider other secondary degrees of freedom which do not determine the change of symmetry but are compatible with it and may be important in the study of the ground state of CaCl_2 . In our particular case, these are easily identified as the amplitude R of the optic mode A_{1g} and the tetragonal strain components $\epsilon_+ = (\epsilon_1 + \epsilon_2)/2$ and ϵ_3 . The eigenvector of the mode A_{1g} has the form $1/\sqrt{8}(000; 000; 110; \bar{1}\bar{1}0; 1\bar{1}0; \bar{1}10)$ (in the same basis used above for the B_{1g} mode). Using these new variables, we can write down a new expansion for E :

$$E = E_0 + \frac{1}{2}\kappa Q^2 + \frac{1}{4}\alpha Q^4 + \frac{1}{2}C_0\epsilon^2 + \gamma Q\epsilon + \gamma' Q^3\epsilon + \frac{1}{2}\delta R^2 + \frac{1}{2}C_+\epsilon_+^2 + \frac{1}{2}C_3\epsilon_3^2 + C_{+3}\epsilon_+\epsilon_3 + aR\epsilon_+ + bR\epsilon_3 + a'RQ^2 + b'\epsilon_+Q^2 + c'\epsilon_3Q^2. \quad (2)$$

Our calculations show that allowed fourth order terms such as $R^4, \epsilon^4, \epsilon_+^4, \epsilon_3^4, Q\epsilon^3$ are not significant and thus have not been included in the previous expansion. We have also checked that the contribution of other higher-order coupling terms is several orders of magnitude smaller than those in Eq. (2). C_+ , C_3 and C_{+3} are bare elastic constants and correspond to $2(C_{11}+C_{12})$, C_{33} and $2C_{13}$, respectively. All the coefficients in the expansion given by Eq. (2) have been determined from ab-initio calculations. δ comes directly from the phonon frequency given in Table II. The bare elastic constants C_+ and C_3 were obtained from the parabolic fit of the total energy for $Q = 0$ versus ϵ_+ and ϵ_3 at $Q = 0$ respectively. The coefficients a and b result from the calculation of the R-conjugate force F_R as a function of ϵ_+ and ϵ_3 respectively, and the elastic constant C_{+3} from the calculation of σ_+ ($\sigma_1 + \sigma_2$) versus ϵ_3 . The coupling coefficient a' is obtained from the parabolic fit of the force F_R as a function of the amplitude Q of the mode B_{1g} . b' and c' are obtained by fitting σ_+ and σ_3 versus the amplitude Q to a parabola. Table III gives a full list of the values obtained for these coefficients.

The resulting energy map can be analyzed in a way similar to that used in the case of Eq. (1). This is evident if we notice that the energy E in Eq. (2) can be rewritten in an equivalent form to that given in Eq. (1) but with the quartic coefficient α renormalized to a smaller value α' given by 0.656 mhartree/bohr⁴ when one introduces the minimum conditions $(\partial E/\partial R)_0 = 0$, $(\partial E/\partial \epsilon_+)_0 = 0$ and $(\partial E/\partial \epsilon_3)_0 = 0$ into Eq. (2). The most important contribution to the renormalization of α comes from the ϵ_+Q^2 coupling term, with almost

TABLE IV: Structural parameters and bulk modulus of the fully relaxed orthorhombic phase of CaCl_2 compared with the experimental values extrapolated to 0 K (Ref. 20). The x and y atomic coordinates for Cl atoms at room temperature are given in lattice units.

	Computed	Experiment	Difference(%)
$a(\text{\AA})$	6.429	6.446	1
$b(\text{\AA})$	6.054	6.167	2
$c(\text{\AA})$	4.088	4.137	1
$x(\text{Cl})$	0.347	0.325	7
$y(\text{Cl})$	0.255	0.275	7
$B_0(\text{GPa})$	31		

90% of the total value. The energy map has three stationary points: the trivial one $Q_0 = 0, \epsilon_0 = 0$ with $E = 0$ which corresponds to a maximum, and the ground state $(Q_m, \epsilon_m) = \pm(1.54 \text{ bohr}, 0.033)$ with $R = -0.01 \text{ bohr}, \epsilon_+ = -0.010, \epsilon_3 = -0.004$ and the depth of the minima $\Delta E = -0.98 \text{ mhartree}$. As expected, the minima are deeper because of a smaller value of the effective quartic coefficient. Furthermore, the ground state values of Q and ϵ have increased, worsening the agreement obtained with experiment when secondary modes were neglected. In fact, the error in the unit cell volume due to the LDA over-binding might be crucial when one considers this issue. The values of ϵ_+ and ϵ_3 can be compared to the experimental ones⁸ extrapolated to 0K ($\epsilon_+ = -0.006$ and $\epsilon_3 = -0.001$).

The deviation from the classical value of the ratio of the slopes of the soft-mode temperature behavior could in principle be related to the secondary strain degrees of freedom analyzed here. As shown above in general, these additional variables renormalize the quartic coefficient α to a lower value α' . When considering secondary spontaneous strains clamped at optical frequencies the slope ratio becomes $r = -2\alpha/\alpha'$. In the present case, for the calculated strain coupling strengths, this could mean a correction of r to about -3 , still very far from the -6.5 observed. On the other hand, these secondary modes or degrees of freedom also affect the calculation done above for the curvature along Q of the ab-initio energy map at the absolute minima and the corresponding ab-initio ground state soft-mode frequency. This becomes 5.34 mhartree/bohr² (3980 cm⁻¹), a huge increase of about 40% with respect to the value obtained disregarding secondary modes (see Fig. 4). This is significantly larger than the extrapolated experimental 0K value. Therefore one can conclude that the comparison with experiment worsens systematically when secondary strain deformations directly related to changes in the unit cell volume are included.

The results obtained above can be compared with the outcome of a direct search for the orthorhombic ground state of CaCl_2 . This comparison also leads to an estimation of the error in the calculations. We minimized the total energy of an orthorhombic unit cell with re-

spect to the volume, allowing for the relaxation of the ratios b/a and c/a and the atomic positions, constrained within the $Pnnm$ space group (two free atomic parameters). The calculated structure is compared in table IV with the experimental orthorhombic structure extrapolated to 0 K. The agreement is very good considering the well known LDA underestimation (the predicted volume of the orthorhombic unit cell is $V_{\text{ort}} = 1075$ bohr 3 , to be compared with the value extrapolated to 0K from experiment (1111 bohr 3)). Using the calculated structural parameters listed in tables I and IV we see that in the absolute orthorhombic minima $\epsilon = 0.030$, $\epsilon_+ = -0.010$ and $\epsilon_3 = -0.007$, which agrees fairly well with the calculated strains from Eq. (2). From the calculated atomic positions of the chlorine atoms we also obtain the amplitude of the B_{1g} mode, $Q = 1.55$ bohr and the A_{1g} mode, $R = -0.06$ bohr. The energy difference between the orthorhombic and tetragonal structures is -0.92 mhartree, to be compared with the depth of the minima, $\Delta E = -0.98$ mhartree, from Eq. (2). Hence, these results are consistent with the ground state that we have found considering the energy expansion given by Eq. (2) with errors of the order of 10%.

VI. ENERGY-VOLUME CURVES AND RELATIVE STABILITY OF DIFFERENT STRUCTURES

We have found it useful to look at the issue of the ferroelastic instability in CaCl_2 from the point of view of the analysis of energy-volume curves, traditional in the field of first-principles calculations. Apart from the consideration of the two phases involved in the transition, a question which comes to mind is whether there might be other structures that could compete for stability with the experimentally observed CaCl_2 structure. A good candidate is the cubic fluorite structure, with the anions placed in a tetrahedral environment and an eightfold coordination of the cations, which is the stable arrangement for the chemically similar compound SrCl_2 .

The calculations in this section are carried out using the the highly accurate all-electron LAPW method, which for the structural properties of CaCl_2 yields essentially the same results as the PW code, as has been shown in Tab. I, but is in principle more suitable to analyze small energy differences between structures. We have computed the energy-volume curves for CaCl_2 in the rutile-type (T), the CaCl_2 -type orthorhombic (O), and the fluorite-type cubic (C) structures, and show them in Fig. 5. The asterisks under C, O, and T mark the equilibrium volumes per formula unit (468, 520, and 535 bohr 3 , respectively).

To put the case of CaCl_2 in perspective, we have performed a similar analysis for SrCl_2 . Fig. 6 shows the total-energy curves for the same three structure-types as for CaCl_2 . The minimum of the total-energy curve for the fluorite-type cubic structure is located at 531 bohr 3 ,

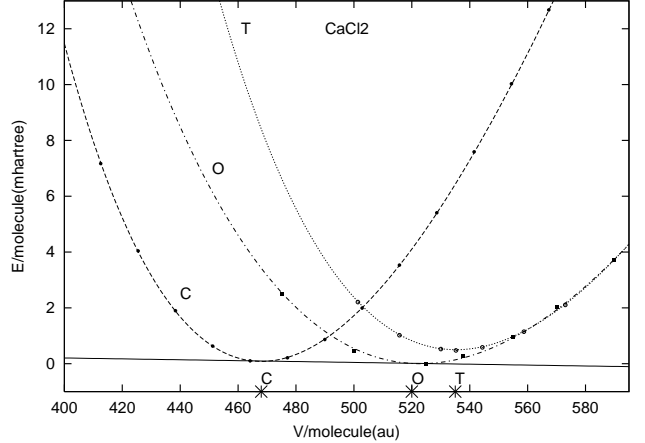


FIG. 5: Total-energy curves for CaCl_2 as a function of the unit cell volume per formula unit (f.u.) for the cubic fluorite-type (C), tetragonal rutile-type (T) and orthorhombic CaCl_2 -type (O) structures. Asterisks mark the volumes per f.u. at the minima. The common tangent of the O and C curves is shown to highlight the very small energy difference between their minima.

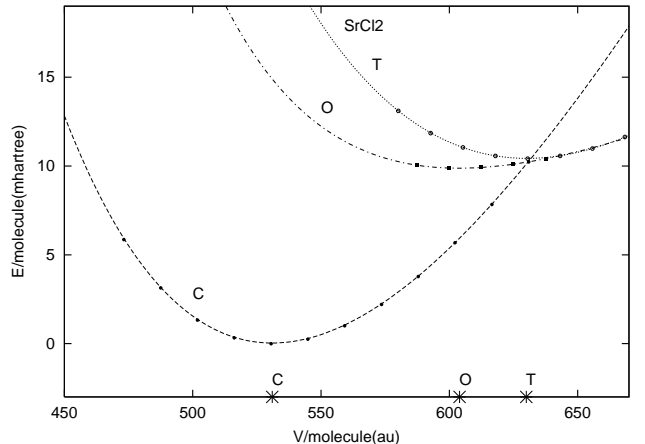


FIG. 6: Total-energy curves for SrCl_2 as a function of the unit cell volume per formula unit (f.u.) for the cubic fluorite-type (C), tetragonal rutile-type (T) and orthorhombic CaCl_2 -type (O) structures. Asterisks mark the volumes per f.u. at the minima.

to be compared with the observed experimental value of 574 bohr 3 . The difference can be attributed to the use of the LDA.

The CaCl_2 -type orthorhombic structure is very similar to the rutile-type tetragonal structure. So, it was to be expected that the energy difference is small both in CaCl_2 and in SrCl_2 (0.48 and 0.54 mhartree/f.u., respectively). In both cases the energies continuously merge as the volume increases, since the B_{1g} optic mode becomes stable and the distortions disappear. This is the signature of a group-subgroup symmetry-breaking transition in an energy-volume diagram. SrCl_2 in the rutile-type structure would have an unstable B_{1g} mode similar to

CaCl_2 , including the negative Grüneisen parameter.

In CaCl_2 , the three structures have very similar energies. The fluorite-type cubic structure is more stable than the rutile-type tetragonal structure (the energy difference is 0.38 mhartree/f.u.). So, the cubic and tetragonal structures are competitive and only the orthorhombic distortion reduces the energy by an additional 0.1 mhartree/f.u. below the cubic one. As shown in Fig. 5, a very small pressure would be enough to transform CaCl_2 into the denser fluorite-type cubic structure. This small energy difference has led us to re-do the calculation with the generalized gradient approximation (GGA) for exchange and correlation.³⁹ In this case the fluorite-type structure is about 8 mhartree/f.u. higher than the tetragonal one, significantly increasing the critical pressure. This finding is consistent with the work of Zupan *et al.*⁴⁰ on the stishovite/alpha-quartz phase transition in SiO_2 , which showed that the compressed phase is too stable within the LDA, whereas the GGA corrects for this over-binding of the LDA and thus agrees better with experiment. In that paper it was argued that it is a general feature of the LDA to favor more compact (isotropic) structures, while the GGA enhances charge inhomogeneities and thus stabilizes the higher-volume and lower-symmetry phase. The present case is another example of this general behavior.

In SrCl_2 , the ground state of the system corresponds to the fluorite-type cubic structure, in accord with the experimental observation. The energy difference with respect to the orthorhombic structure (within the LDA) is 9.88 mhartree/f.u., much larger than in the case of CaCl_2 . This can be understood by considering the non-bonding forces between the cations. The corresponding potential grows steeply at short distances due to strong repulsive forces. For this reason the relative energies are sensitive to the first-neighbor Ca-Ca and Sr-Sr distances. In SrCl_2 the cations in the tetragonal structure are very close to each other and thus raise the total energy. In CaCl_2 , however, the cations are not so close and thus the corresponding energy difference between the structures is relatively small.

VII. CONCLUSIONS

Ab-initio calculations within the LDA approximation without volume corrections are sufficient to reproduce the main features of the ferroelastic instability in CaCl_2 . Our analysis of the energetics of the crystal confirm a pseudoproper ferroelastic mechanism with an unstable optic mode as the microscopic origin of the experimental phase transition. The elastic instability arises due to the coupling between this soft B_{1g} optic mode and the orthorhombic spontaneous strain ϵ . The existence of QRUMs in the rutile-type framework structure has been shown to play an essential role as well. The calculated orthorhombic ground state agrees fairly well with the experimental low temperature structure. We have identified and calculated the anharmonic terms which have relevance in the determination of the ground state. The secondary degrees of freedom have been also considered. Our energy-map calculations rule out the relevance of higher anharmonic couplings proposed in previous literature to explain the ratio of the slopes of the squared frequencies. Although the system modifies its ground state noticeably when volume/strain corrections are considered, the LDA approximation has been sufficient for obtaining a realistic picture of the microscopic mechanism of this temperature driven ferroelastic system.

Acknowledgments

This work was supported in part by the UPV research grants 060.310-EA149/95 and 063.310-G19/98, and by the Spanish Ministry of Education grant PB98-0244. We gratefully acknowledge valuable discussions with E.K.H. Salje and K. Parlinski and helpful comments from J. Íñiguez and S. Ivantchev. We are also indebted to M. T. Dove for his help with the program CRUSH. J.A.V. was supported by the Spanish Ministry of Education and appreciates the warm hospitality at the TU in Vienna during the realization of part of this work.

* Electronic address: wdpagaara@lg.ehu.es

¹ W. Zhong, D. Vanderbilt and K.M. Rabe, Phys. Rev. Lett. **73**, 1861 (1994).

² U.V. Waghmare and K.M. Rabe, Phys. Rev. B **55**, 6161 (1997).

³ D. Vanderbilt and W. Zhong, Ferroelectrics **206** (1-4), 181 (1998).

⁴ M.G. Stachiotti, G. Fabricius, R. Alonso and C. O. Rodriguez, Phys. Rev. B **58**, 8145 (1998).

⁵ R.E. Cohen and H. Krakauer, Phys. Rev. B **42**, 6416 (1990).

⁶ J.A. Válgora, J.M. Pérez-Mato and A. García, Ferroelectrics **237**, 377-384 (2000).

⁷ H.-G. Unruh, D. Mühlberg and Ch. Hahn, Z.Phys.B-Condensed Matter **86**, 133 (1992).

⁸ H.-G. Unruh, Phase Transitions, **45**, 77 (1993).

⁹ P. Hohenberg and W. Kohn, Phys. Rev. **136**, 864B (1964).

¹⁰ W. Kohn and L.J. Sham, Phys. Rev. **140**, 1133A (1965).

¹¹ J.P. Perdew and A. Zunger, Phys. Rev. B **23**, 5048 (1981).

¹² D.M. Ceperley and B.J. Alder, Phys. Rev. Lett. **45**, 566 (1980).

¹³ N. Troullier and J.L. Martins, Phys. Rev. B **43**, 1993 (1991).

¹⁴ H.J. Monkhorst and J.D. Pack, Phys. Rev. B **13**, 5188, (1976).

¹⁵ D. Vanderbilt and S.G. Louie, Phys. Rev. B **30**, 6118 (1984).

¹⁶ P. Blaha, K. Schwarz and J. Luitz, WIEN97, Vienna University of Technology 1997. [Improved and updated Unix version of the original copyrighted WIEN code, which was

published by P. Blaha, K. Schwarz, P. Sorantin and S.B. Trickey, *Comput. Phys. Commun.* **59**, 339 (1990).]

¹⁷ J.P. Perdew and Y. Wang, *Phys. Rev. B* **45**, 13244 (1992).

¹⁸ B. Kohler, S. Wilke, M. Scheffler, R. Kouba and C. Ambrosch-Draxl, *Comp. Phys. Commun.* **94**, 31 (1996).

¹⁹ F.D. Murnaghan, *Proc. Nat. Acad. Sci. U.S.A.* **30**, 244 (1944).

²⁰ B. Anselment: Thesis, Universität Karlsruhe 1986.

²¹ M. O'Keeffe, *Acta Cryst. A* **33**, 924 (1977).

²² P.I. Sorantin and K. Schwarz, *Inorg. Chem.* **31**, 567 (1992).

²³ W.H. Weber, G.W. Graham and J.R. McBride, *Phys. Rev. B* **42**, 10969 (1990).

²⁴ A. Perakis, E. Sarantopoulou, Y.S. Raptis and C. Raptis, *Phys. Rev. B* **59**, 775 (1999).

²⁵ D. Andrault, G. Fiquet, F. Guyot and M. Hanfland, *Science*, **282**, 720 (1998).

²⁶ J.D. Jorgensen, T.G. Wrolton and J.C. Jamieson, in *High Pressure Science and Technology, Proceedings of the 6th AIRAPT Conference on High Pressure*, edited by K. D. Timerhans and M. S. Barber (Plenum, New York, 1979), vol.1, p.152.

²⁷ J. Haines, J.M. Léger, C. Chateau, R. Bini and L. Ulivi, *Phys. Rev. B* **58**, 2909 (1998) and references therein.

²⁸ A.K.A. Pryde, K.D. Hammonds, M.T. Dove, V. Heine, J.D. Gale and M.C. Warren, *J. Phys.: Condens. Matter* **8**, 10973 (1996).

²⁹ A.P. Giddy, M.T. Dove, G.S. Pawley and V. Heine, *Acta Cryst. A* **49**, 697 (1993).

³⁰ K.D. Hammonds, M.T. Dove, A.P. Giddy and V. Heine, *Am. Mineral.* **79**, 1207, (1994).

³¹ B.B. Karki, M.C. Warren, L. Stixrude, G.J. Ackland and J. Crain, *Phys. Rev. B* **55**, 3465 (1997).

³² G.A. Samara and P.S. Peercy, *Phys. Rev. B* **7**, 1131 (1973).

³³ P.S. Peercy and B. Morosin, *Phys. Rev. B* **7**, 2779 (1973).

³⁴ J. Pascual, J. Camassel, P. Merle, B. Gil and H. Mathieu, *Phys. Rev. B* **24**, 2101 (1981).

³⁵ S. Radescu, I. Etxebarria and J.M. Perez-Mato, *J. Phys.: Condens. Matter* **7**, 585 (1995).

³⁶ J.M. Perez-Mato, S. Ivantchev, A. García, I. Etxebarria, *Ferroelectrics* **236**, 93-103 (2000).

³⁷ G.H.F. van Raaij, K.J.H. van Bemmel and T. Janssen, *Phys. Rev. B* **62**, 3751 (2000)

³⁸ J.M. Perez-Mato, I. Etxebarria, S. Radescu and S. Ivantchev, *Eur. Phys. J. B* **12**, 331 (1999).

³⁹ We use the scheme in J. Perdew, K. Burke and M. Ernzerhof, *Phys. Rev. Lett.* **77**, 3865 (1996).

⁴⁰ A. Zupan, P. Blaha, K. Schwarz and J. Perdew, *Phys. Rev. B* **58**, 11266 (1998).